FLUORIDE
Quarterly reports

ADSORPTION OF RADIOFLUORINE ^{18}F IONS ONTO METAL ORGANIC FRAMEWORK

Unique digital address (Digital object indentifier[DOI} equivalent):
https://www.fluorideresearch.online/epub/files/229.pdf

Thaer Assaad[1], Bassem Assfour[2]

[1]Department of Radioisotope, Atomic Energy Commission of Syria (AECS), P.O. Box 6091, Damascus, Syrian Arab Republic.
[2]Department of Chemistry, Atomic Energy Commission of Syria (AECS), P. O. Box 6091, Damascus, Syrian Arab Republic

***Corresponding author:**
Bassem Assfour; Department of Chemistry, Atomic Energy Commission of Syria (AECS), P. O. Box 6091, Damascus, Syrian Arab Republic.
Phone: +963(11) 2132580; Fax: +963(11) 6112289;
E-mail: cscientific@aec.org.sy, bassfour@aec.org.sy

Accepted: 2023 Jun 15
Epub as e229: 2023 Oct 26

ABSTRACT

Fluoride is one of the drinking water contaminants regulated by the World Health Organization. The reduction of fluoride concentration to a safe range is of paramount importance to human life. Moreover, the fast and high-capacity removal of radioactive ^{18}F wastes is still challenging. Metal organic frameworks (MOFs) are a hybrid class of materials that can diminish such contaminants via both adsorption and catalysis processes. In this work, we synthesize three different MOFs and study their adsorption behavior towards fluoride ion removal. The synthesized materials were characterized using X-ray diffraction, FT-IR and scanning electron microscopy. Following investigation we showed that the as-synthetized materials were highly stable and had significantly effective fluoride adsorption performance What is more, the activity of fluoride captured by the material Al-Fu MOF is 603 µCi in 40 mg of this material, i.e., the removal efficiency is about 98%.

Key-words: Radio fluoride; MOFs; XRD; IR; Removal efficiency

INTRODUCTION

Fluoride is an important pollutant in drinking water in many countries around the globe[1]. The World Health Organization (WHO) recommended upper limit of fluoride in drinking water is 1.5 mg/L, which is also the upper limit for fluoride in drinking water for several other countries such as Canada, India, Australia, and the European Union, although it also allows countries to set their own country standards, such as Senegal having a country standard of 0.6 mg/L[2]. The low dosage of fluoride in drinking water is considered by many to be helpful for dental health[3], but an excessive intake, most commonly with drinking-water, can cause serious health problems, such as fluorosis of teeth (dental fluorosis) and bones (skeletal fluorosis) and nonskeletal fluorosis, such as reduced IQ[4]. Therefore, the reduction of fluoride concentration to the allowed range is urgently necessary.

In nuclear medicine, Fluorine is used as a radioactive tracer in positron emission tomography (PET) scans mostly as Fluorodeoxyglucose (FDG), which is similar to glucose and is taken up at a higher rate by brain and cancer cells[5]. A cyclotron can produce ^{18}F mainly by bombarding ^{18}O, a stable natural isotope of oxygen, with protons (^{1}H). The target materials used can be either in the solid, liquid or gas phase. Depending on the form of the target, either ^{18}F ion in water or ^{18}F–F$_2$ gas is obtained. ^{18}F–F$_2$ gas can also be made by shooting deuterons at Ne target[6]. However, radiofluorine ^{18}F has a short half-life of about 110 minutes and decays into oxygen ^{18}O, which emits a positron and a neutrino. This means that radiofluorine ^{18}F can pose a radiation hazard to the environment and human health if it is not properly disposed of after use. Therefore, it is necessary to separate and remove radiofluorine ^{18}F ions from aqueous solutions before they are discharged into water bodies or landfills. Solid alumina is routinely used for the separation and removal of ^{18}F from the solid target in cyclotron[7].

Kheradpisheh et al.[8] investigated the impact of drinking water fluoride on human thyroid hormones, specifically thyroxine (T3), triiodothyronine (T4), and thyroid stimulating hormone (TSH). The study found that even low levels of fluoride in drinking water can have an impact on TSH values, leading to an impairment of thyroid function. They recommended the use of standard household water purification systems for patients with hypothyroidism to remove fluoride that interferes with thyroid functions. They also identified several other variables associated with hypothyroidism, including gender, family history, exercise, diabetes, hypertension, and water consumption.

Yousefi and co-workers[9] found a significant link between fluoride intake from drinking water and hypertension in people living in fluoride endemic areas in Iran. People who drank water with high fluoride levels had higher odds of hypertension than those who drank water with lower fluoride levels. Age, sex, BMI, and fluoride level in drinking water were significantly associated with increased blood pressure. However, fluoride did not have significant associations with BMI, hip circumference, and waist to hip ratio. These findings were very relevant for healthcare workers and drinking-water policymakers.

The fluoride levels and health effects of drinking water from 28 villages in Poldasht city, Iran, were examined by Yousefi et al.[10]. The fluoride content varied from 0.27 to 10.3 mg/L (average 1.70 mg/L) in the water samples. More than half of the samples exceeded the fluoride limit for drinking water. The health risk assessment showed that young consumers, children, and teenagers in different regions of Poldasht city were exposed to the highest fluoride levels. The study recommended reducing fluoride concentration in drinking water and preventing fluorosis. It also urged regular monitoring of fluoride levels to protect the population from potential risk.

The fluoride levels in drinking water sources and the DMFT (Decayed, Missing and Filled Teeth) index in 12-year-old students in Behshar city were investigated by Mahvi et al.[11]. They surveyed 300 students and tested 120 water samples. The results indicated that the average fluoride concentration of drinking water for one year was 0.25 ppm, which is below the normal level. The average DMFT value was 1.48±0.13 and was higher for girls than for boys. The study recommended considering other fluoride sources in planning public health dentistry programs. The study provided useful data on the DMFT prevalence and fluoride levels in drinking water sources in Behshar city.

Metal organic frameworks (MOFs) are highly porous crystals with a great potential as functional materials of many applications in the future[12,13]. Some MOFs have the ability to capture and store voluminous amounts of gas molecules (i.e., CH_4, H_2, N_2 and CO_2)[14]. The fact that structure of MOFs can be tailored and chemically functionalized to selectively adsorb a specific gas in a mixture gives them an enormous advantage over other nano porous materials. Furthermore, MOFs have a versatile ability to store and release gases with fast kinetics and high reversibility over multiple cycles. Despite some technical obstacles, MOF containing membranes have great potential in environmental restoration application. MOF-containing membranes can be applied for water purification[15,16]. MOFs-based adsorbents have been frequently examined for the removal of organic[17] and metal ions[18] pollutants from aqueous solutions. The unique properties of MOFs, such as tuneable porosities, large pore volumes, hierarchical structures, excellent adsorption, and regeneration performances attracted significant research interest in water treatment. The major interaction mechanisms between MOFs and organic pollutants in response to numerous experimental conditions, such as pH, temperature, and coexisting ions[19] have been intensively investigated. Some conclusions and recommendations were drawn for designing MOFs with improved adsorption performances.

Recently, MOFs have been successfully used to reduce the concentration of fluoride in both drinking and wastewater to safe ranges[20-22]. Some MOFs have been reported to show high fluoride removal capacity and selectivity, such as Al-MOFs[23], Zr-MOFs[24,25], and Fe-MOFs[26]. The adsorption mechanism of fluoride by MOFs involves electrostatic attraction, ligand exchange, and hydrogen bonding. However, there are also some challenges and limitations for using MOFs for fluoride removal, such as water stability, regeneration, and cost[24]. Therefore, more research and development are needed to optimize the performance and applicability of MOFs for fluoride removal from water.

In recent years, the application of MOFs in the nuclear field has been significantly increased[27-30.] MOFs were used as sorbents for various gaseous and anionic radioactive species such as $^{129/131}I_2$, ^{127}Xe, ^{85}Kr, $^{235/238}UO_2^{2+}$, $^{232}Th^{4+}$, $^{137}Cs^{+}$, $^{90}Sr^{2+}$, $^{99}TcO_4^{-}$ (ReO_4^{-}), $^{79}SeO_3^{2-}$ and $^{79}SeO_4^{2-}$ [31,32]. For instance, Qasem et al. have successfully synthesized and characterized four new MOFs and tested them for Iodine (I_2) adsorption in both vapor and liquid phases. Their results indicated that Iodine adsorbs in MOF structure as I_2 and I_3^- due to the presence of π rings in the MOFs[33]. It is well known that the radioisotope ^{99}Tc combines the feature of long half-life and large fission yield, which make it one of the most challenging radioisotopes in the nuclear industry. Sheng et al. have successfully synthesized a novel cationic MOF denoted by SCU-100. SCU-100 structure consists of 1D channels filled with unbound nitrate anions, in addition to coordination Ag^+ cations as potential open metal sites. This material was examined to remove TcO_4^- anion from aqueous solution. It showed excellent properties in both kinetic and quantitative removal of TcO_4^-, and it was better than other functional materials used for the same application[34]. Later on, Kang and co-workers have synthesized new Nickel-based cationic MOFs (ZJU-X6), which exhibited high efficiency and selectivity toward removal of radioactive $^{99}TcO_4^-$ from aqueous solution. Results showed that $^{99}TcO_4^-$ trapped in the materials structure through coordination with Ni^{2+} atoms, In addition to various hydrogen bonding with organic ligands.

In this paper, we extend the work on MOFs to examine radio fluoride capture and separation in three different MOFs with different metal ions, pore size and topology. The results of this work may provide useful information to unlock the potential of these materials in storage and separation applications of ionic radioisotopes and help designing new adsorbents with improved properties by studying the effect of material structure on adsorption properties.

The three selected MOFs in this study are three of the most studied MOFs in the literature, they are MIL-101(Cr), MIL-53 (Al), Al-Fu MOF. The crystal structures of these materials are shown in Figures 1A–1C.

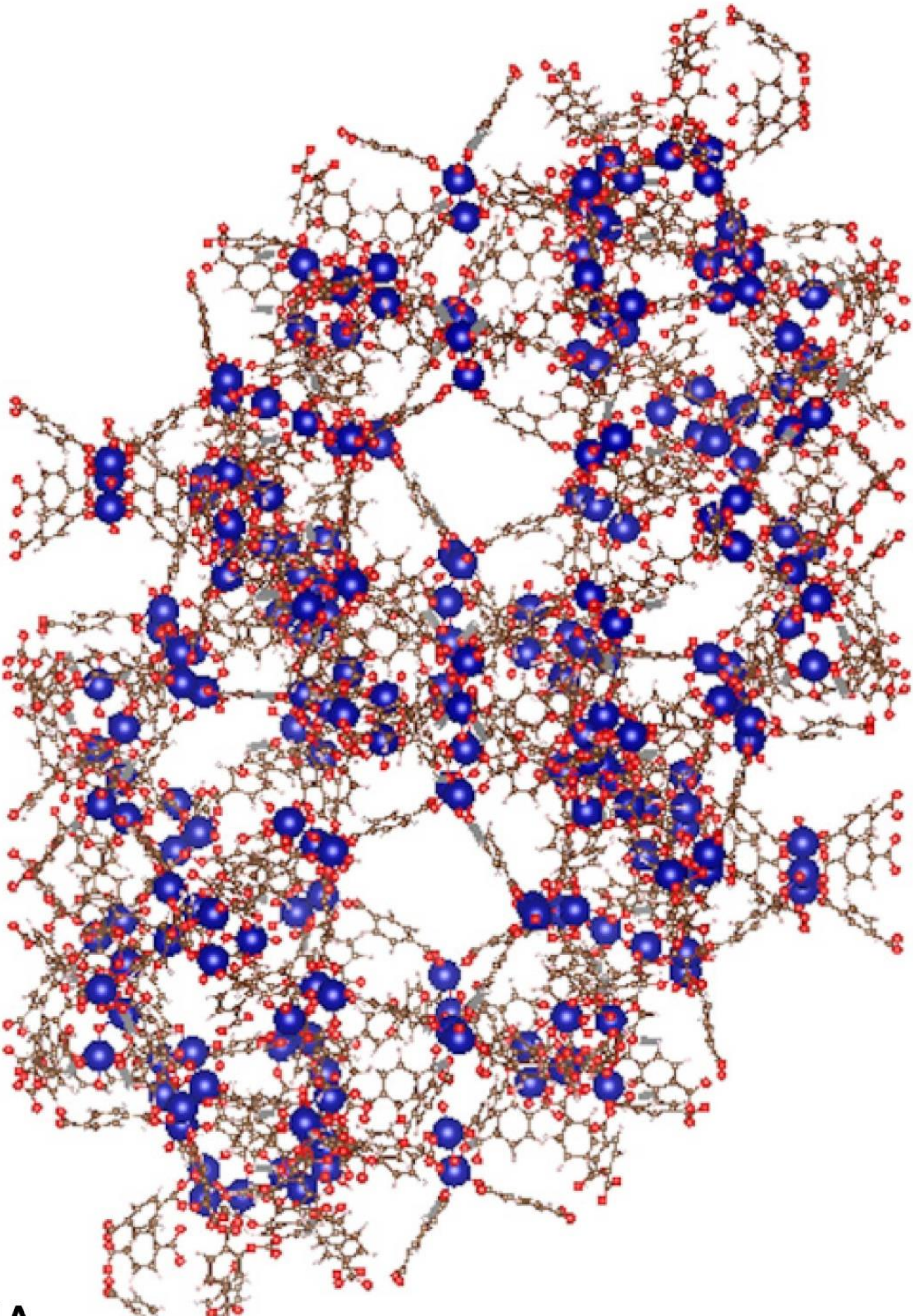

Figure 1A. Crystal structures of the MOFs studied in this work. 1A: MIL-101-Cr MOF (Cr, dark blue; O, red; C, gray; H, white; Al, pink). (For interpretation of the references to color in this fig legend, the reader is referred to the web version of this article).

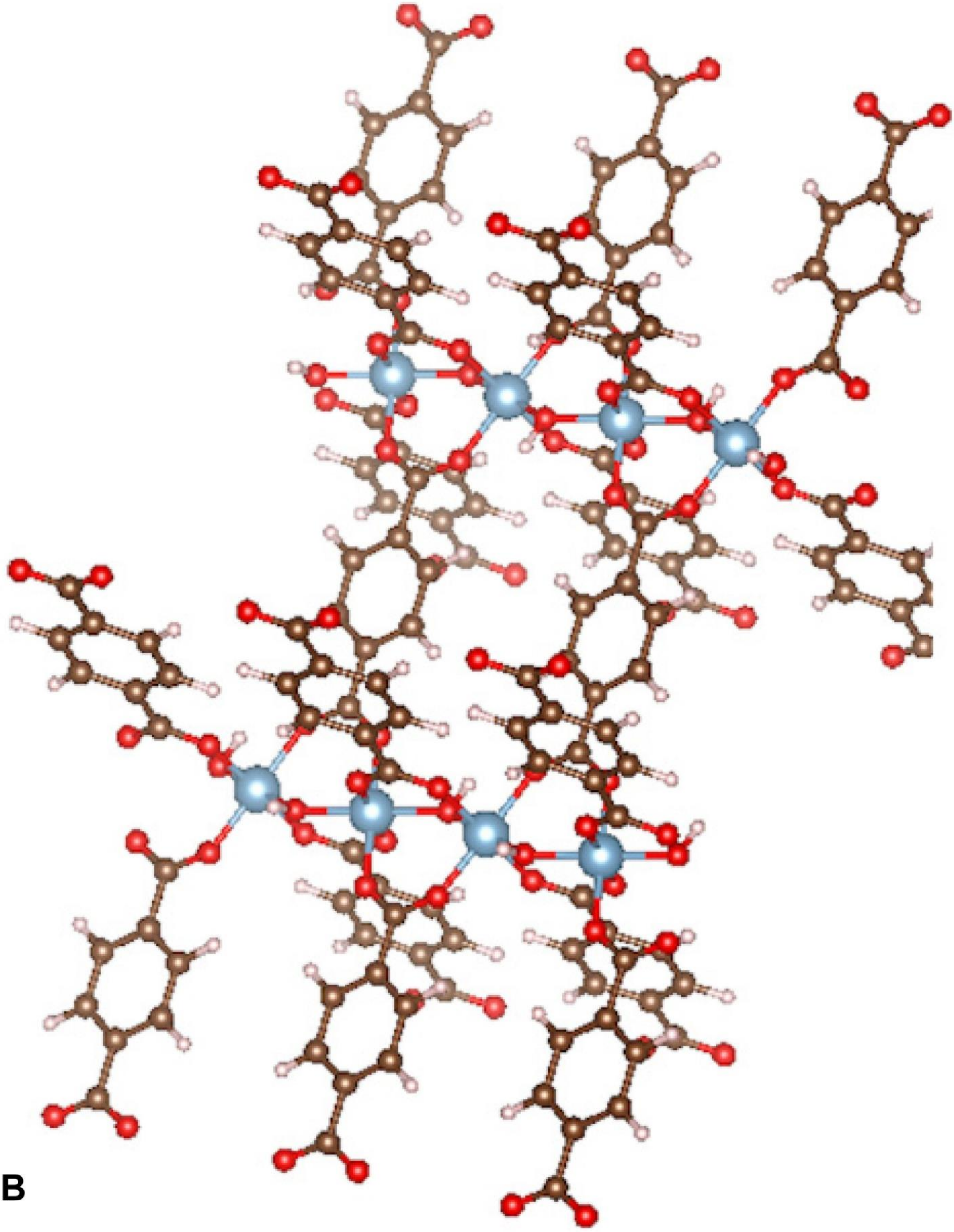

1B

Figure 1B. Crystal structures of the MOFs studied in this work. 1B: MIL-53-Al MOF (Cr, dark blue; O, red; C, gray; H, white; Al, pink). (For interpretation of the references to color in this fig legend, the reader is referred to the web version of this article).

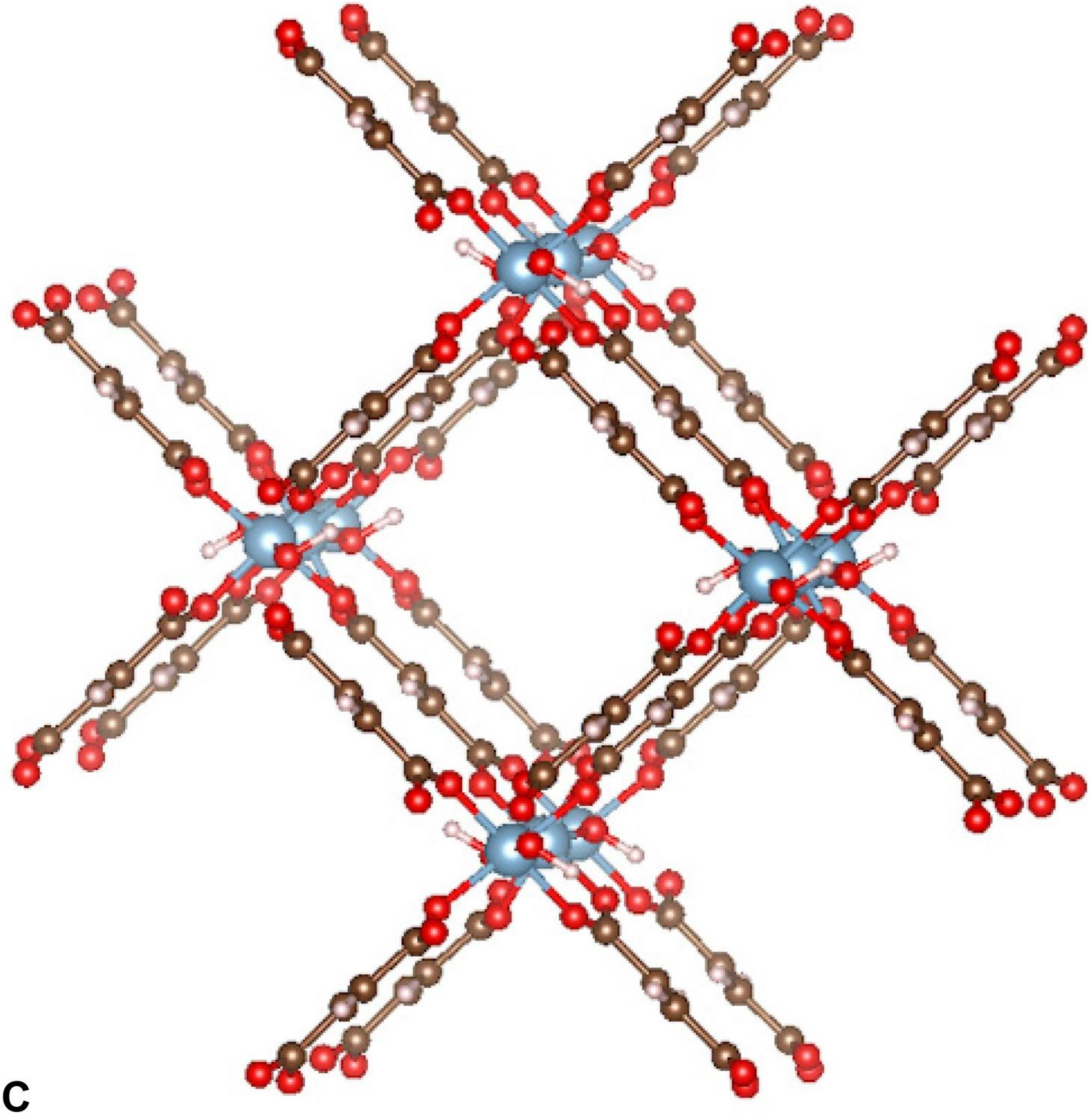

1C

Figure 1C. Crystal structures of the MOFs studied in this work. 1C: Al-Fu MOF (Cr, dark blue; O, red; C, gray; H, white; Al, pink). (For interpretation of the references to color in this fig legend, the reader is referred to the web version of this article).

MATERIAL AND METHODS

All chemical reagents and solvents were of commercial quality and used as received. Infrared spectra were recorded as KBr pellets in the range 400–4000 cm^{-1} using an FTIR-JASCO 300E. The X-ray powder diffraction (XRD) patterns were obtained using a StoeStadi-P diffractometer with monochromatic Cu K·1 radiation (λ=1.5406 Å) selected using an incident-beam curved-crystal germanium Ge (111) monochromator, using the Stoe transmission geometry (horizontal set-up) with a linear position-sensitive detector (PSD). The Scanning electron microscopy SEM were obtained using OnTescan Vega II XMU SEM.

^{18}F was provided as commercial available kit produced by Atomic Energy Commission of Syria. In a hot cell, A solution of Na^{18}F (306 mCi, 601 mCi, 511 mCi in 1ml) was passed into 3 filters contain 40 mg (newly activated) of MIL-101(Cr), MIL-53(Al) and Al-Fu MOF respectively. After total filtration the radioactivity of the filter was measured using gamma detector and the percentage of the uptake radiofluorine in the filter was determined using the relation:

$$\% \, CI = \frac{AF}{AV0-AV} \; {*}100$$

Where:

%CI: Percentage of radioactive fluorine, detained in filters

AV_0 (mCi): Activity of vial (radiofluorine used)

AV (mCi): Activity of vial after filtration process

AF (mCi): Activity of filter after filtration process.

The synthesis, purification and activation of MIL-101(Cr) were explained in detail in our previous work[35]. MIL-53(Al) was synthesized by a solvothermal method using aluminum nitrate as the aluminum source and 1,4-benzenedicarboxylic acid (H2BDC) as the organic ligand. according to the same method of Mil 101 synthesis with some modifications. Briefly, a mixture of 800 mg (2mmol) aluminum nitrate and 332 mg (2mmol) Terephthalic acid and 40 mg (2 mmol) Hydrofluoric in 10 ml distilled water was heated at 200 ºC for 8 h in a Teflon-lined stainless steel reactor. After cooling, the product was separated from water by centrifugation at 5000 rpm for 10 minutes. In order to remove the incorporated terephthalic acid, the white solid precipitate was first washed 2–3 times with distilled water and then 1 time with methanol and acetone respectively. Finally the product was treated with N,Ndimethylformamide (DMF) at 70 ºC for 21 hours, after that the suspension was centrifuged at 5000 rpm for 10 minutes, the product was washed again with methanol and acetone respectively, then heated at 75 ºC for 21h. Activation of MIL-53(Al) was carried out by drying under vacuum at 100 ºC for 12 h. Al-Fu MOF was synthesized using aluminum sulphate 18 hydrate ($Al_2(SO_4)_3{}^{2}18H_2O$) and fumaric acid according to the method described in the literature with some modifications[36]. 18.55 g of $Al_2(SO_4)_3\cdot 18H2O$ was added to 79.5 ml of water in a round bottom flask and heated at 60 ºC for one hour. Another solution consisting of 4.75 g NaOH and 6.45 g fumaric acid in 95.5 ml water was added to the solution at 60 ºC for two hours with slow stirring. After cooling, a white precipitate of aluminum fumarate was formed and separated out by centrifugation at 5000 rpm for 10 minutes. The precipitate was washed 5 to 6 times with distilled water and then 1 time with methanol and acetone respectively, the material was dried in a vacuum oven at 100 ºC for 24 h. The Al-Fu MOF obtained using this method was around 3.0 g. Activation of Al Fu MOF was carried out by drying under vacuum at 150 o C for 5 h and then at 180 ºC for 2 h.

RESULTS

1. Characterization of MIL-101(Cr), MIL-53(Al) and Al-Fu MOF

The compounds were characterized using X-ray scattering technique in order to match the crystalline structures of the synthesized materials with the expected structures by comparing the experimental X-ray scattering spectrum for each material with the theoretical spectrum calculated from the crystal structure of the material. Image of the manufactured materials were also taken using a scanning electron microscope in order to determine the grain size of the formed crystal structures. Figures 2A–2C shows the experimental and theoretical X-ray scattering spectrum for (2A) MIL-101(Cr), (2B) MIL-53(Al), and (2C) Al-Fu MOF.

We noticed from the comparison between the experimental spectrum (black blank dots) and the theoretical spectrum (the solid blue line) for the three materials, a correspondence between the locations of the peaks and the relative intensities, which indicates the formation of the structures required for the three materials. The difference between the experimental and theoretical spectrum (especially in the material MIL-53) results from many reasons, the most important of which are: the lack of complete crystallization of the material and not completely getting rid of the solvent used during the synthesizing process, as some particles remain stuck in the nano-pores of the material in addition to the presence of some impurities which share some peaks in the combined spectrum.

The morphology of the manufactured materials were determined using scanning electron microscope (SEM) images based on the signals given by the atoms in the sample. In general, 3 to 5 images were taken for each sample using SEM. The process is set up so that the image is random and covers all ranges of sizes in the sample. Figures 3–5 show SEM images taken from samples at different magnifications. In general, we notice the presence of crystals of different sizes, where the crystal dimensions range between 100–500 nm for (Figure 3) MIL-101 (Cr), 5–10 µm for MIL-53 (Figure 4) and 50–100 nm for (Figure 5) Al-Fu MOF. The particle size of the manufactured materials in our case is similar to that reported in the literature for other MOFs materials with the exception of MIL-53 which exhibits a large particle size compared to other MOFs materials. Particle size is affected by many factors such as nucleation, crystal growth and super saturation. In the case of MIL-53 the activation energy of crystal growth is higher than that of crystal growth, and the increase in the temperature of the reaction components when synthesizing the material leads to a reduction in solution super saturation by increasing the solubility and as a result, large-sized granules are obtained.

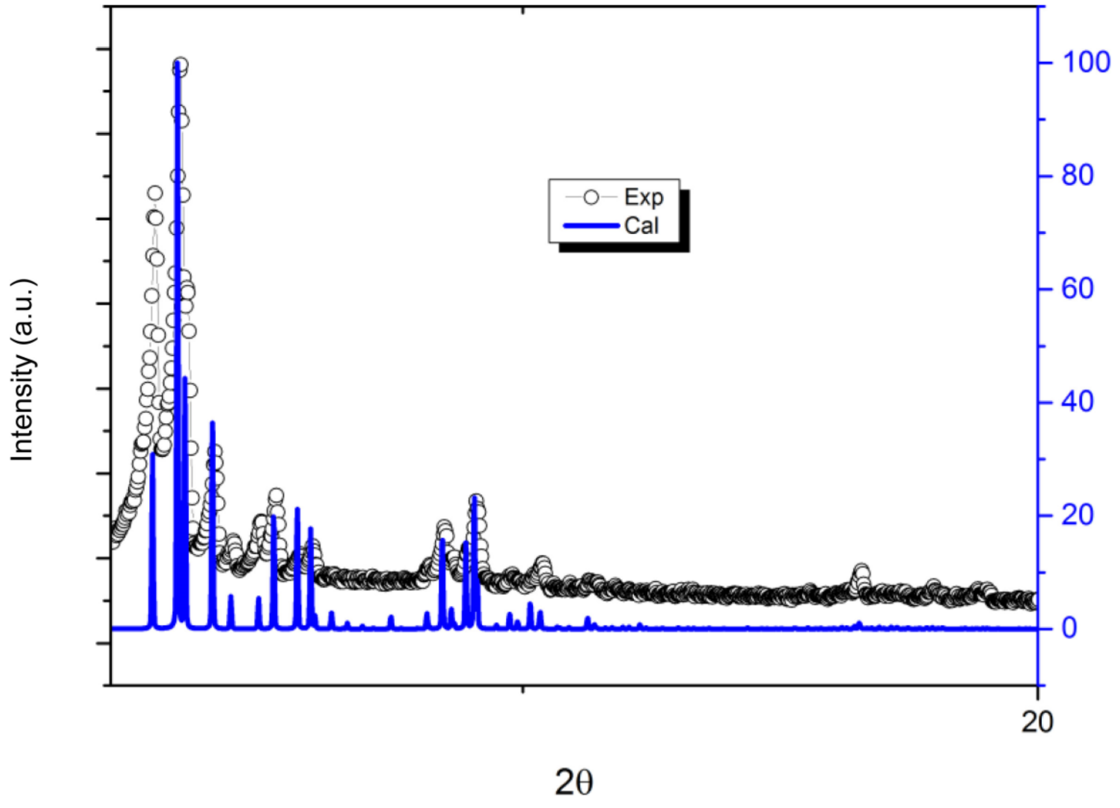

2A

Figure 2A. Experimental (blank dots) and theoretical (blue solid line) X-ray spectrum of materials. 2A: MIL-101 (Cr).

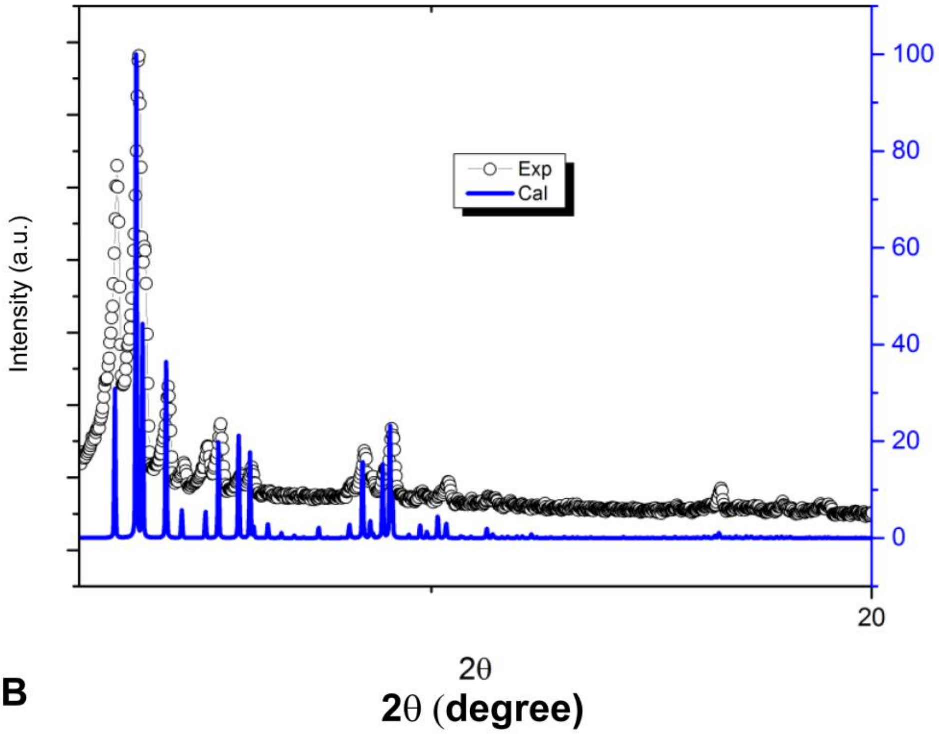

2B

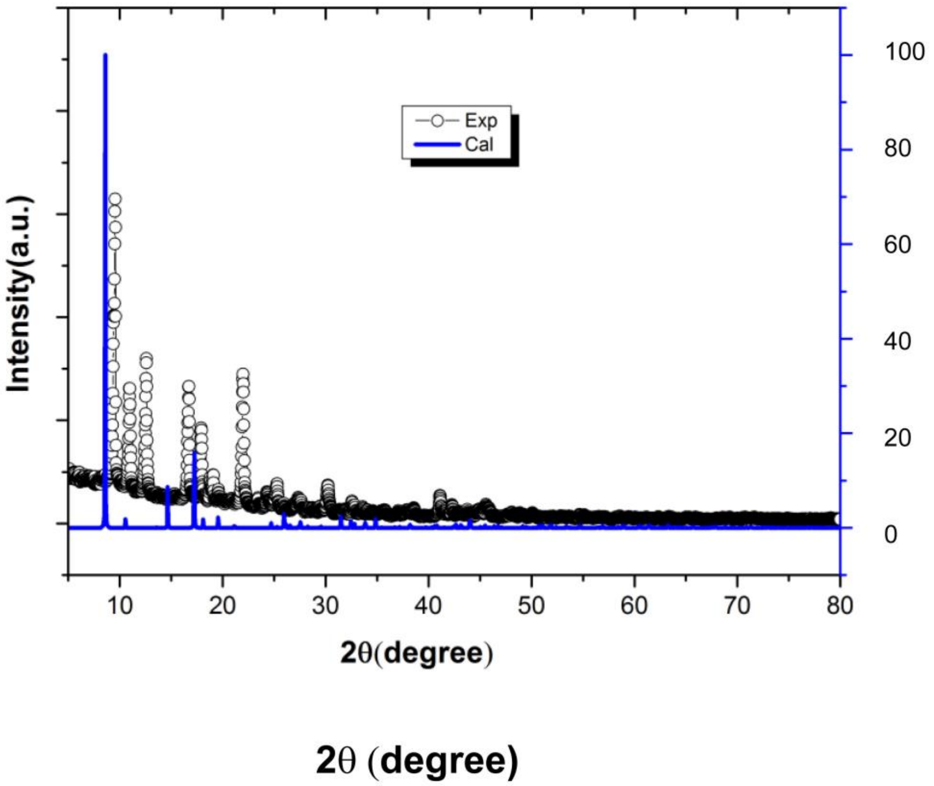

2C

Figures 2B and 2C. Experimental (blank dots) and theoretical (blue solid line) X-ray spectrum of materials. 2B: MIL-53(Al); 2C: Al-Fu MOF.

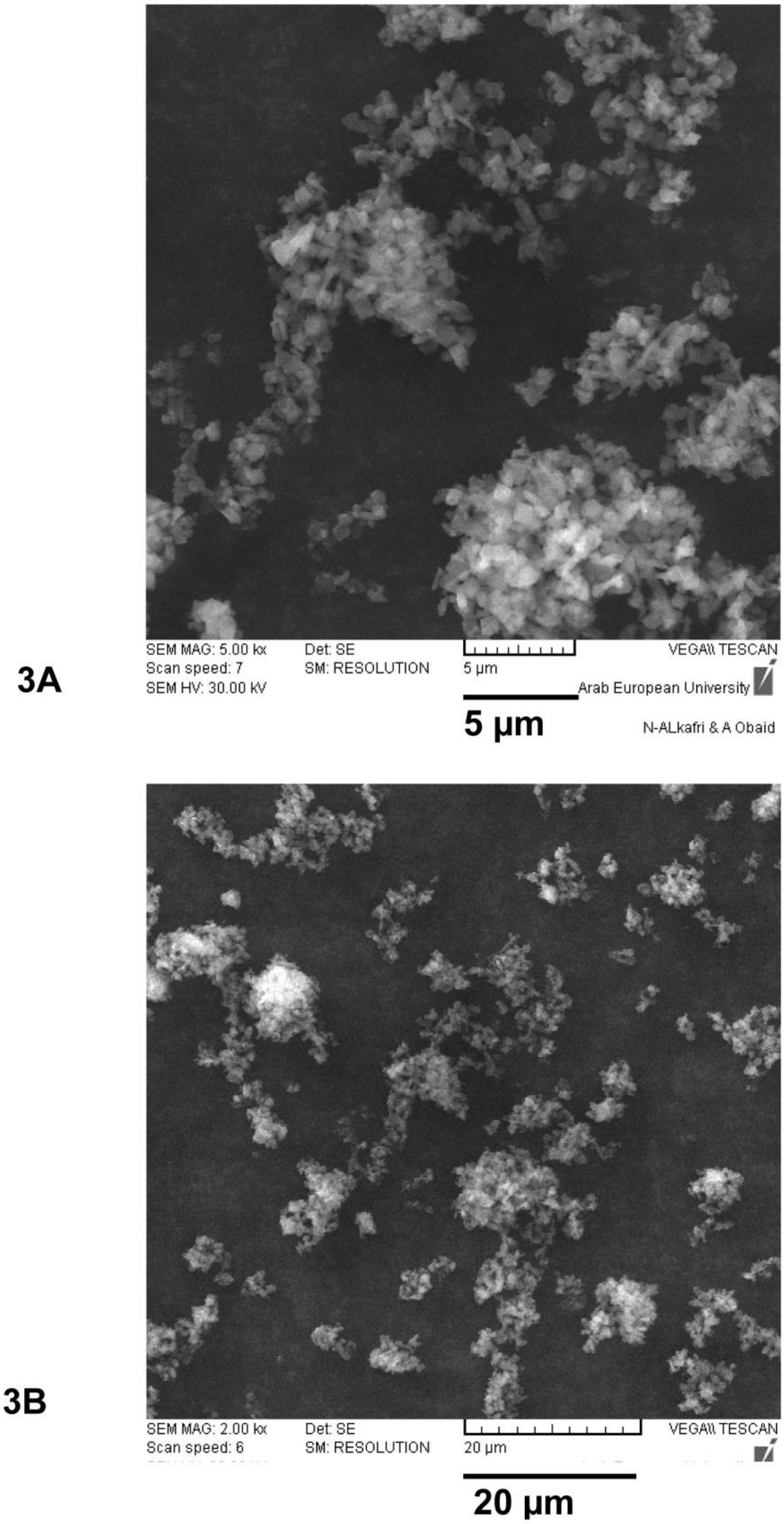

Figures 3A and 3B. SEM images of the MIL-101 sample with different magnifications.

3C

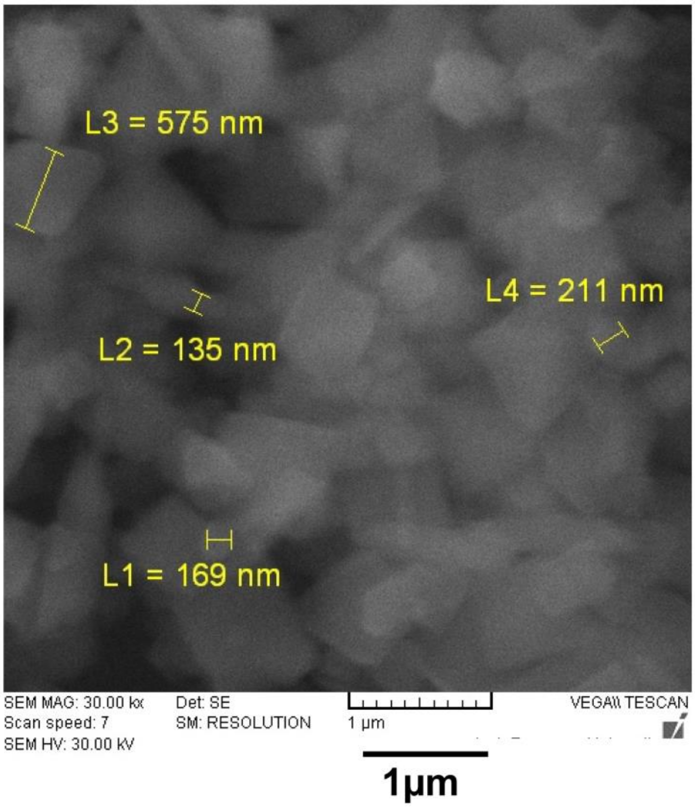

3D

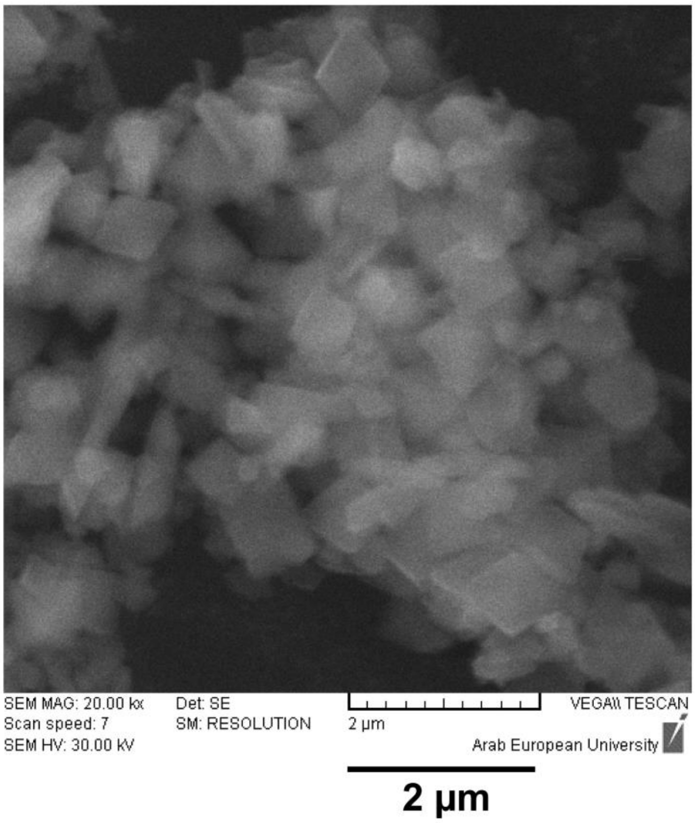

Figures 3C and 3D. SEM images of the MIL-101 sample with different magnifications.

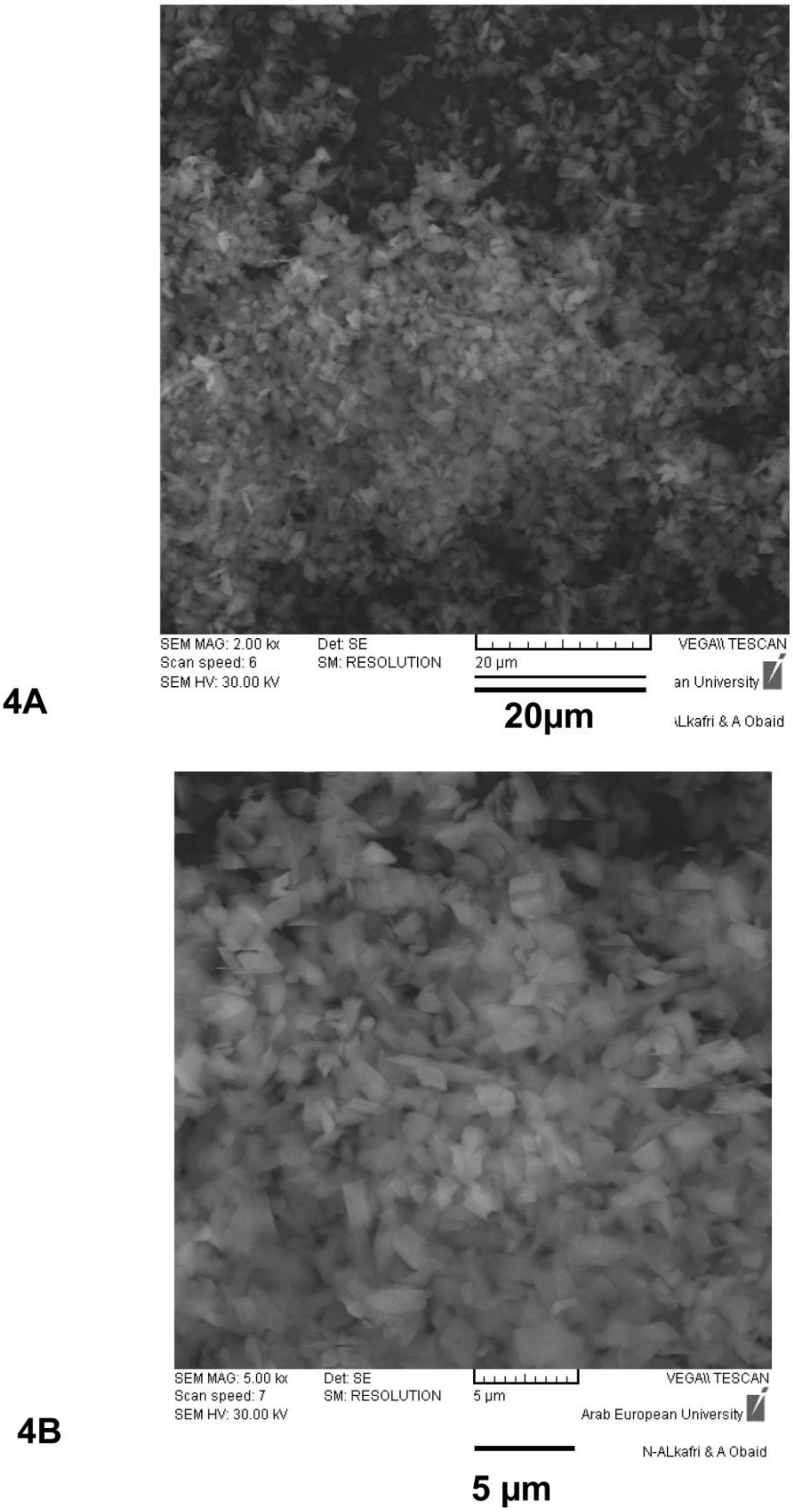

Figures 4A and 4B. SEM images of the MIL-53 sample with different magnifications.

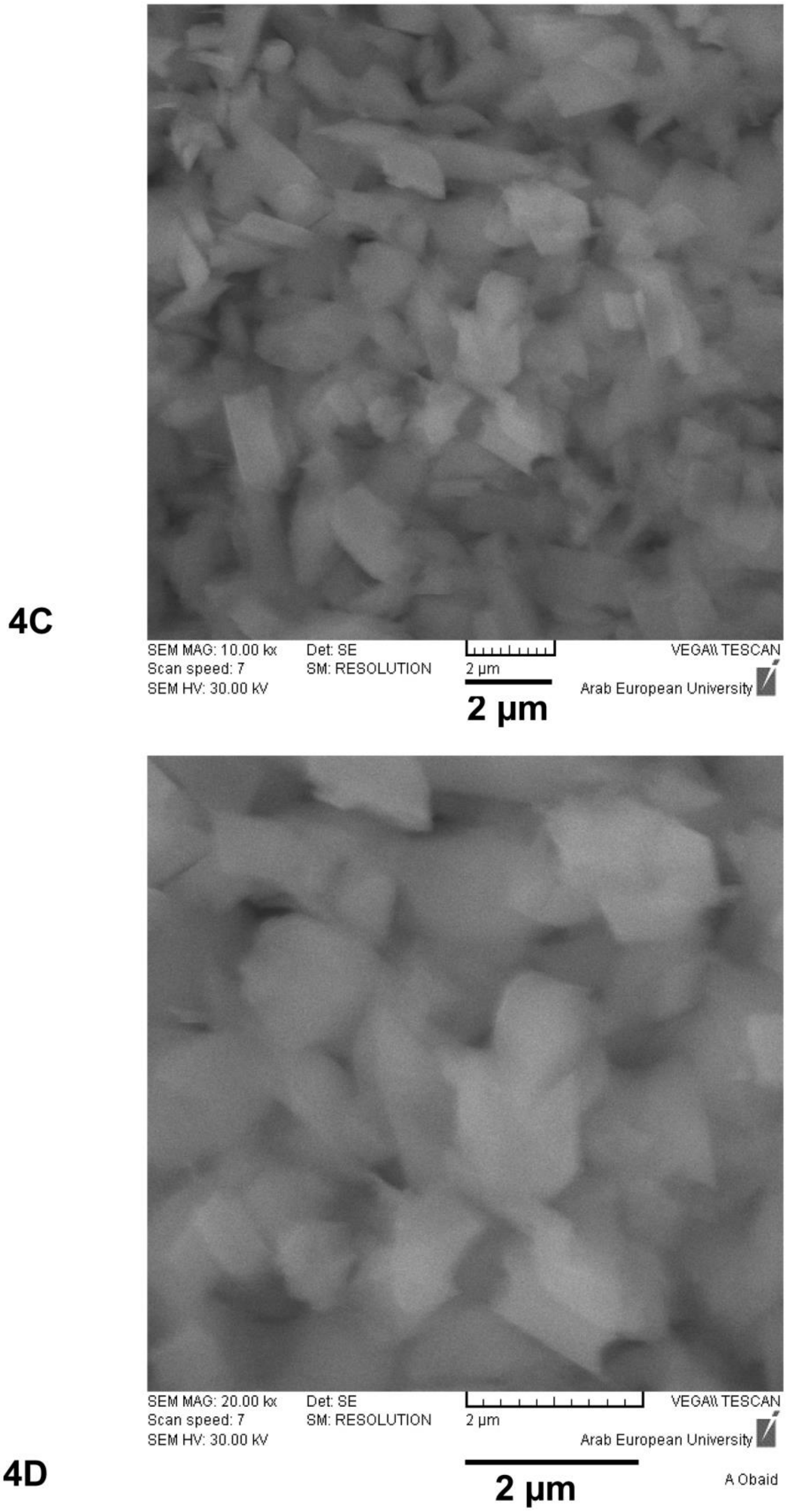

Figures 4C and 4D. SEM images of the MIL-53 sample with different magnifications.

5A

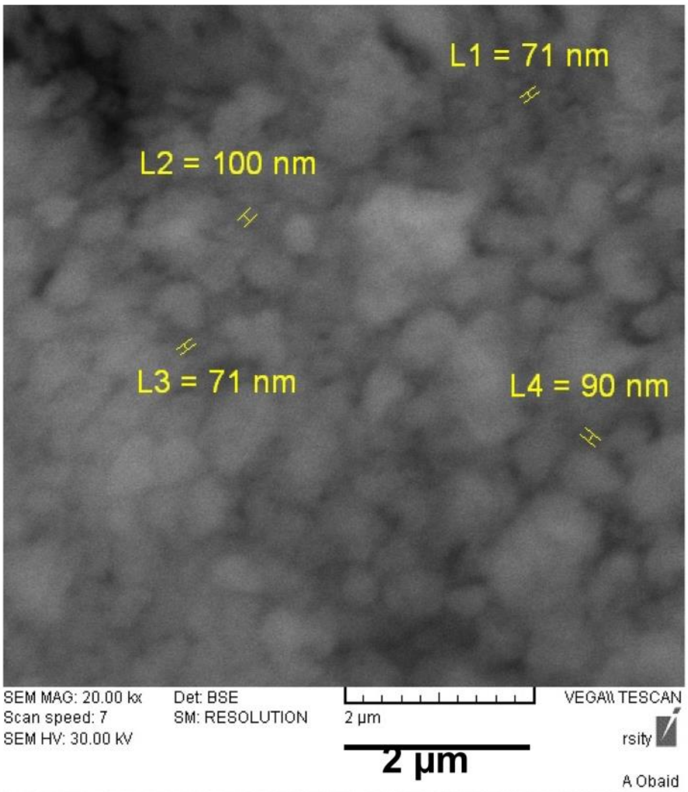

5B

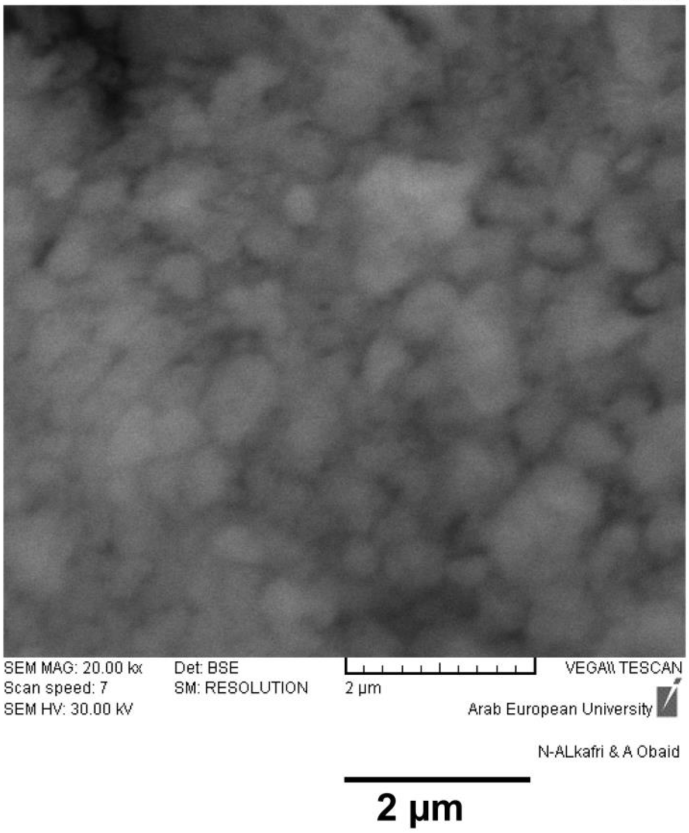

Figures 5A and 5B. SEM images of the Al-Fu MOF sample with different magnifications.

5C

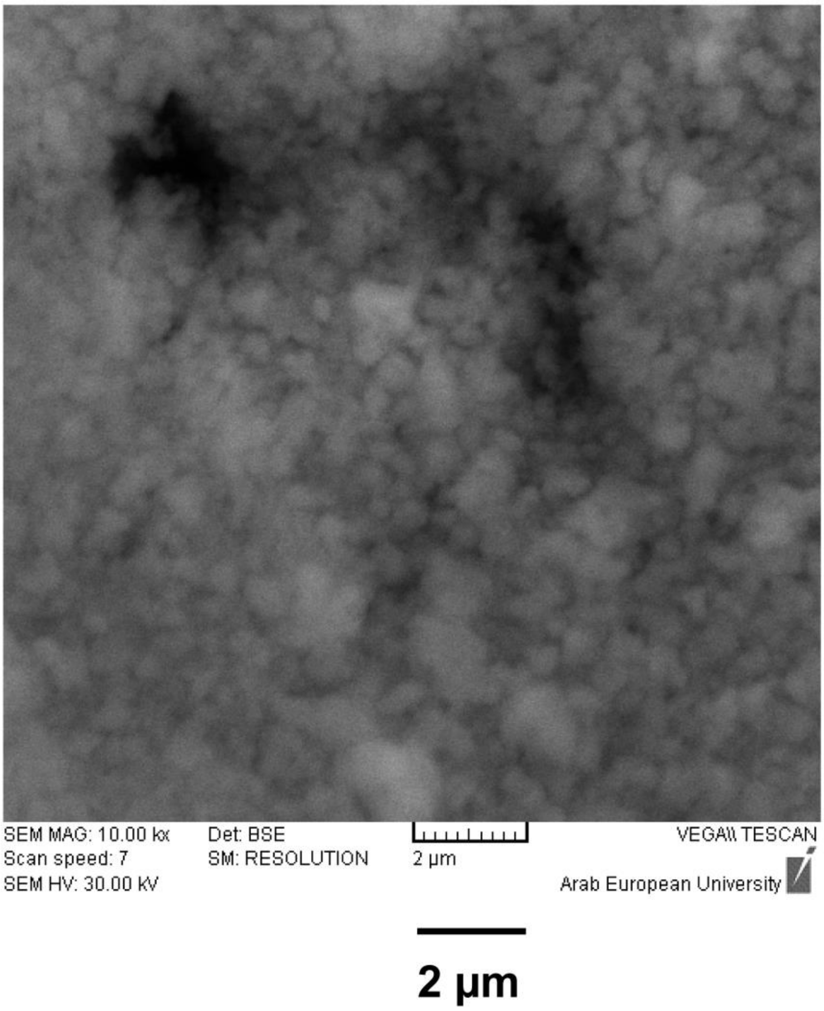

Figure 5C. SEM image of the Al-Fu MOF sample with a different magnification.

The characteristic FTIR bands of MIL-101(Cr) were explained in details in our previous work[35]. These bands included the C = C stretching vibration at 1505 cm^{-1}, the C-H deformation vibration at 1160, 1018, 884, and 750 cm^{-1}, and the characteristic bands of framework –O–(C = O)– groups at 1430 and 1555 cm^{-1} [37]. In addition, the most intense signals at 1385 and 1555 cm^{-1} were ascribed to the stretching vibration for the carboxylates. (See Figure 6) The IR spectra (Figure 7) of MIL- 53 (Al) exhibit vibrational bands in the usual region of 1695 cm^{-1} for the carboxylic function. two absorption bands, located at 1597 and 1509 cm^{-1}, can be assigned to -CO_2 asymmetric stretching, whereas bands at 1439 and 1414 cm^{-1} can be assigned to -CO_2 symmetric stretching. These values are consistent with the presence of CO_2 groups that are coordinated to aluminum. Figure 8 shows FTIR analysis taken for Al-Fu MOF. In general, we observed that the Al-OH stretch and the OH stretch at 577 and 3705 cm^{-1}. two absorption bands, located at 1613 and 1475 cm^{-1}, can be assigned to -CO_2 asymmetric stretching.

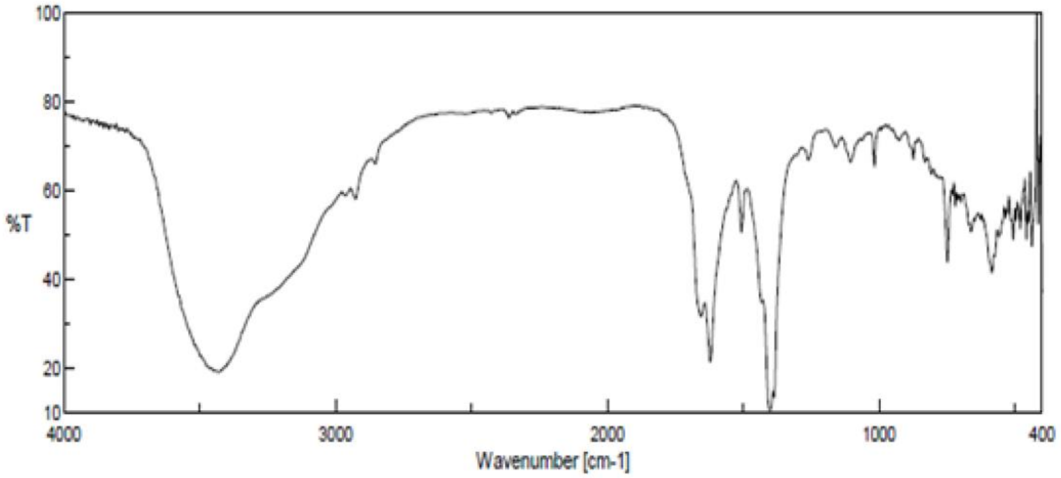

Figure 6. FTIR spectrum of MIL-101

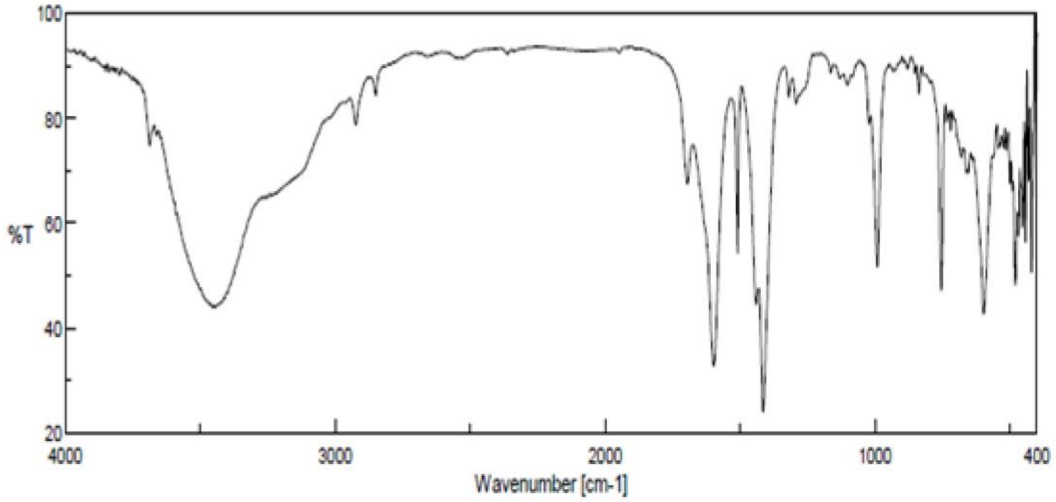

Figure 7. FTIR spectrum of MIL-53.

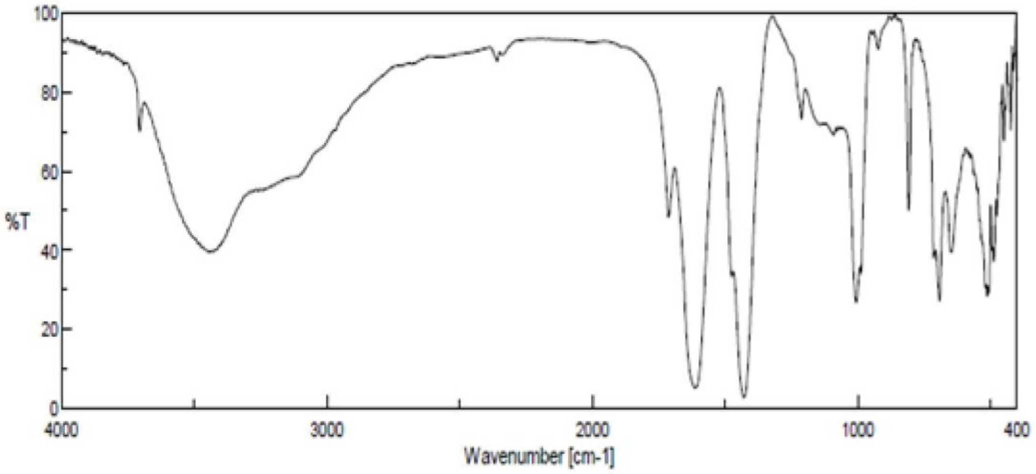

Figure 8. FTIR spectrum of Fu MIL.

2. Radiofluorine-18 Adsorption

Table 1 summarizes the measurements of radioactivity of the three filters containing MOFs before and after ^{18}F Filtration. Results showed that 40 mg of Al-Fu MOF can adsorb 98% (603 µCi) of radiofluorine ^{18}F. Same experiment was repeated in same conditions using MIL-101(Cr), MIL-53(Al) in the filter as reference compound. The results showed that the capture of radioactive fluorine on the MIL-101(Cr), MIL53(Al) filters were 68.6 and 86.84%, respectively. Therefore, Al-Fu MOF can be used as candidate agent for radio-fluorine capture in hot cells.

Table 1. Radioactivity of the three filters containing MOFs before and after ^{18}F Filtration

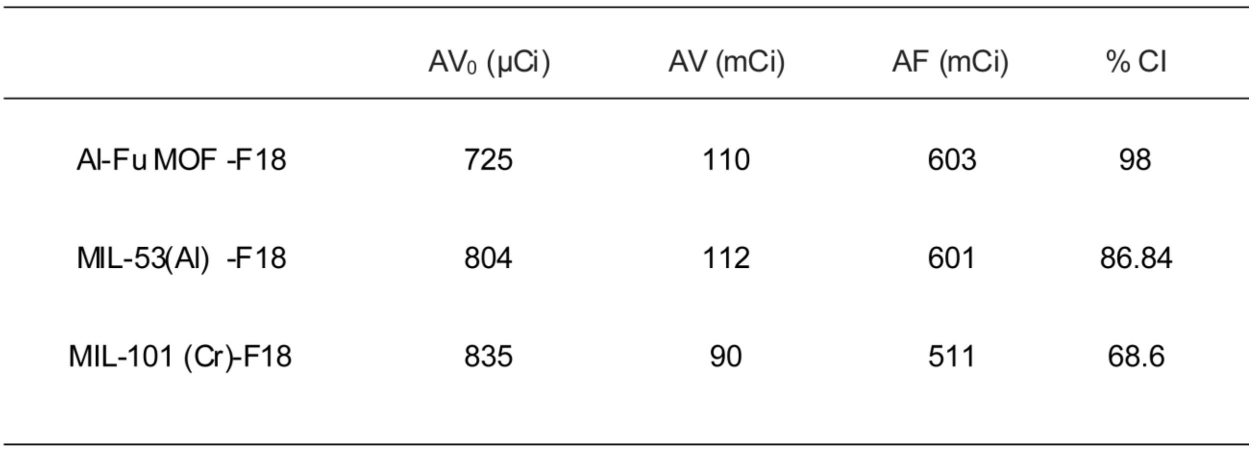

	AV$_0$ (µCi)	AV (mCi)	AF (mCi)	% CI
Al-Fu MOF -F18	725	110	603	98
MIL-53(Al) -F18	804	112	601	86.84
MIL-101 (Cr)-F18	835	90	511	68.6

CONCLUSIONS

In this work, experimental study was conducted for the possibility of using MOF compounds in the applications of capturing radioactive fluorine ions. Three MOFs of different metal clusters, topology and pore size were selected and synthesized. The resulting compounds were characterized using different techniques, and then the adsorption of radioactive fluorine on these materials was studied. The results showed the large ability of some of these compounds to capture fluorine ions, where the amount of activity captured in the material Al-Fu MOF About 603 µCi in about 40 mg of this substance (98%).

ACKNOWLEDGEMENTS

The authors thank Prof. I. Othman; the Director General of the Atomic Energy Commission of Syria for his valuable assistance. Thanks, are also due to N. Daouud, Zeinab Aje, T. Saleh, K. Latifi, N. Al Kafri, R. Ajayan for technical support.

CONFLICT OF INTERESTS

The authors reported no conflict of interest

REFERENCES

[1] Huang L, Wan K, Yan J, Wang L, Li Q, Chen H, Zhang H, Xiao T. Nanomaterials in Water Applications: Adsorbing Materials for Fluoride Removal. 2021. Vol. 11, Page 1866. https://doi.org/10.3390/nano11071866

[2] Tao W, Zhong H, Pan X, Wang P, Wang H, Huang L. Removal of fluoride from wastewater solution using Ce-AlOOH with oxalic acid as modification. Journal of hazardous materials 2020, 384:121373. DOI: 10.1016/j.jhazmat.2019.121373

[3] Kanduti D, Sterbenk P, Artnik B. Fluoride: a review of use and effects on health. Materia socio-medica 2016, 28:133. DOI: 10.5455/msm.2016.28.133-137

[4] Tian YQ, Chen ZX, Weng LH, Guo HB, Gao S, Zhao DY. Two polymorphs of cobalt(II) imidazolate polymers synthesized solvothermally by using one organic template N,Ndimethylacetamide. Inorganic Chemistry 2004, 43:4631-4635. DOI: 10.1021/ic049713z

[5] Le Bars D. Fluorine-18 and medical imaging: Radiopharmaceuticals for positron emission tomography. Journal of fluorine chemistry 2006, 127:1488-1493. DOI: 10.1016/ j.jfluchem.2006.09.015

[6] Jacobson O, Kiesewetter DO, Chen X. Fluorine-18 Radiochemistry, Labeling Strategies and Synthetic Routes. Bioconjugate Chemistry 2015, 26:1-18, doi:10.1021/bc500475e.

[7] International Atomic Energy A. Cyclotron Produced Radionuclides: Guidance on Facility Design and Production of [18F] fluorodeoxyglucose (FDG): IAEA; 2012.

[8] Kheradpisheh Z, Mirzaei M, Mahvi AH, Mokhtari M, Azizi R, Fallahzadeh H, Ehrampoush MH. Impact of Drinking Water Fluoride on Human Thyroid Hormones: A Case- Control Study. Scientific Reports 2018, 8:2674, doi:10.1038/s41598-018-20696-4.

[9] Yousefi M, Yaseri M, Nabizadeh R, Hooshmand E, Jalilzadeh M, Mahvi AH, Mohammadi AA. Association of hypertension, body mass index, and waist circumference with fluoride intake; water drinking in residents of fluoride endemic areas, Iran. Biological trace element research 2018, 185:282-288.

[10] Yousefi M, Ghoochani M, Hossein Mahvi A. Health risk assessment to fluoride in drinking water of rural residents living in the Poldasht city, Northwest of Iran. Ecotoxicology and Environmental Safety 2018, 148:426-430, doi:https://doi.org/10.1016/ j.ecoenv.2017.10.057.

[11] Mahvi A, Zazouli M, M Y, Nikpour B, A B. Survey of Fluoride Concentration in Drinking Water Sources and Prevalence of DMFT in the 12 Years Old Students in Behshar City. Journal of Medical Sciences 2006, 6, doi:10.3923/jms.2006.658.661.

[12] Cui Y, Li B, He H, Zhou W, Chen B, Qian G. Metal–organic frameworks as platforms for functional materials. Accounts of chemical research 2016, 49:483-493.

[13] Chen Z, Kirlikovali KO, Li P, Farha OK. Reticular Chemistry for Highly Porous Metal–Organic Frameworks: The Chemistry and Applications. Accounts of chemical research 2022, 55:579-591.

[14] Connolly BM, Madden DG, Wheatley AEH, Fairen-Jimenez D. Shaping the future of fuel: Monolithic metal–organic frameworks for high-density gas storage. Journal of the American Chemical Society 2020, 142:8541-8549.

[15] Bedia J, Muelas-Ramos V, Peñas-Garzón M, Gómez-Avilés A, Rodríguez JJ, Belver C. A review on the synthesis and characterization of metal organic frameworks for photocatalytic water purification. Catalysts 2019, 9:52.

[16] Yu S, Pang H, Huang S, Tang H, Wang S, Qiu M, Chen Z, Yang H, Song G, Fu D. Recent advances in metal-organic framework membranes for water treatment: a review. Science of The Total Environment 2021, 800:149662.

[17] Tchinsa A, Hossain MF, Wang T, Zhou Y. Removal of organic pollutants from aqueous solution using metal organic frameworks (MOFs)-based adsorbents: A review. Chemosphere 2021, 284:131393, doi:https://doi.org/10.1016/j.chemosphere.2021.131393.

[18] Zadehahmadi F, Eden NT, Mahdavi H, Konstas K, Mardel JI, Shaibani M, Banerjee PC, Hill MR. Removal of metals from water using MOF-based composite adsorbents. Environmental Science: Water Research & Technology 2023, 9:1305-1330, doi:10.1039/ D2EW00941B.

[19] Yan C, Jin J, Wang J, Zhang F, Tian Y, Liu C, Zhang F, Cao L, Zhou Y, Han Q. Metal– organic frameworks (MOFs) for the efficient removal of contaminants from water: Underlying mechanisms, recent advances, challenges, and future prospects. Coordination Chemistry Reviews 2022, 468:214595, doi:https://doi.org/10.1016/j.ccr.2022.214595.

[20] Yang Y, Li X, Gu Y, Lin H, Jie B, Zhang Q, Zhang X. Adsorption property of fluoride in water by metal organic framework: Optimization of the process by response surface methodology technique. Surfaces and Interfaces 2022, 28:101649, doi:https://doi.org/10.1016/j.surfin.2021.101649.

[21] Huang Q, Zhao L, Zhu G, Chen D, Ma X, Yang X, Wang S. Outstanding performance of thiophene-based metal-organic frameworks for fluoride capture from wastewater. Separation and Purification Technology 2022, 298:121567.

[22] Zhu L, Zhang C, Wang L, Zhang J. The simple synthesis of metal organic frameworks with high fluoride adsorption performance from water. Journal of Solid State Chemistry 2022, 307:122866, doi:https://doi.org/10.1016/j.jssc.2021.122866.

[23] Tang X, Zhou C, Xia W, Liang Y, Zeng Y, Zhao X, Xiong W, Cheng M, Wang Z. Recent advances in metal–organic framework-based materials for removal of fluoride in water: Performance, mechanism, and potential practical application. Chemical Engineering Journal 2022, 446:137299, doi:https://doi.org/10.1016/j.cej.2022.137299.

[24] Ahmadijokani F, Molavi H, Rezakazemi M, Aminabhavi TM, Arjmand M. Simultaneous detection and removal of fluoride from water using smart metal-organic frameworkbased adsorbents. Coordination Chemistry Reviews 2021, 445:214037, doi:https://doi.org/10.1016/j.ccr.2021.214037.

[25] Zhu X-H, Yang C-X, Yan X-P. Metal-organic framework-801 for efficient removal of fluoride from water. Microporous and Mesoporous Materials 2018, 259:163-170, doi:10.1016/j.micromeso.2017.10.001.

[26] Zhou G, Meng Q, Li S, Song R, Wang Q, Xu Z, Xing Z. Novel magnetic metal-organic framework derivative: An adsorbent for efficient removal of fluorine-containing wastewater in mines. Journal of Environmental Chemical Engineering 2022, 10:108421, doi:https://doi.org/10.1016/j.jece.2022.108421.

[27] Assfour B, Assaad T, Odeh A. In silico screening of metal organic framework for iodine capture and storage. Chemical Physics Letters 2014, 610:45-49.

[28] Al Lafi AG, Assfour B, Assaad T. Metal organic framework MIL-101 (Cr): Spectroscopic

investigations to reveal Iodine capture mechanism. Journal of Inorganic and Organometallic Polymers and Materials 2020, 30:1218-1230.

[29] Assaad T, Assfour B. Metal organic framework MIL-101 for radioiodine capture and storage. Journal of Nuclear Materials 2017, 493:6-11.

[30] Al Lafi AG, Assfour B, Assaad T. Spectroscopic investigations of gamma-ray irradiation effects on metal organic framework. Journal of Materials Science 2021, 56:12154- 12170.

[31] Jin K, Lee B, Park J. Metal-organic frameworks as a versatile platform for radionuclide management. Coordination Chemistry Reviews 2021, 427:213473, doi:https://doi.org/ 10.1016/j.ccr.2020.213473.

[32] Patra K, Ansari SA, Mohapatra PK. Metal-organic frameworks as superior porous adsorbents for radionuclide sequestration: Current status and perspectives. Journal of Chromatography A 2021, 1655:462491, doi:https://doi.org/10.1016/ j.chroma.2021.462491.

[33] Qasem KMA, Khan S, Ahamad MN, Saleh HAM, Ahmad M, Shahid M. Radioactive iodine capture by metal organic frameworks in liquid and vapour phases: An experimental, kinetic and mechanistic study. Journal of Environmental Chemical Engineering 2021, 9:106720, doi:https://doi.org/10.1016/j.jece.2021.106720.

[34] Sheng D, Zhu L, Xu C, Xiao C, Wang Y, Wang Y, Chen L, Diwu J, Chen J, Chai Z, et al. Efficient and Selective Uptake of TcO4– by a Cationic Metal–Organic Framework Material with Open Ag+ Sites. Environmental Science & Technology 2017, 51:3471- 3479, doi:10.1021/acs.est.7b00339.

[35] Assaad T, Assfour B. Metal organic framework MIL-101 for radioiodine capture and storage. Journal of Nuclear Materials 2017, 493:6-11, doi:http://dx.doi.org/10.1016/ j.jnucmat.2017.05.036.

[36] Assfour B, Abadllah B, Kakhia M. Synthesis and Characterization of ZnS/PbS Quantum Dots Nanorods Array Heterostructure. Aerosol Science and Engineering 2022, 6:215- 222.

[37] Al Lafi AG, Assfour B, Assaad T. Metal Organic Framework MIL-101(Cr): Spectroscopic Investigations to Reveal Iodine Capture Mechanism. Journal of Inorganic and Organometallic Polymers and Materials 2020, 30:1218-1230, doi:10.1007/s10904-019- 01236-7